RSC Advances

PAPER

View Article Online
View Journal | View Issue

Cite this: *RSC Adv.*, 2026, **16**, 24870

Photocatalytic prins-like indole addition of tryptophol C2 with aldehydes and ketones

Lanxiang Liu,[abc] Yunfeng Tao,[b] Menghan Chu,[b] Xiaojian Zhou,[b] Guanben Du,[b] Bei Zhou *[ab] and Jun Lin *[a]

Received 10th December 2025
Accepted 15th April 2026

DOI: 10.1039/d5ra09558a

rsc.li/rsc-advances

Introducing functional groups at the C2 position of indole is useful and important for the synthesis of complex indole-based pharmaceuticals and polymeric materials. In this study, a novel photocatalytic Prins-like indole addition was developed, enabling cross-coupling between the C2 position of tryptophol and carbonyl groups of aldehydes and ketones. This reaction was facilitated by an intramolecular ligand-to-metal charge transfer (LMCT) process initiated through cerium-based photocatalysis, which excited an indole alkanol to generate an alkoxy radical. This alkoxy radical promoted selective cleavage of the indole C2 sp^2 C–H bond *via* a 1,5-hydrogen atom transfer (1,5-HAT) pathway, thereby forming a carbon-centered radical at the C2 position. The resulting carbon radical subsequently underwent nucleophilic addition to aldehydes or ketones, affording secondary alcohols from aldehydes and tertiary alcohols from ketones. This article describes an efficient photocatalytic radical-based transformation analogous to the Prins reaction and provides a practical synthetic approach for constructing alcohol functionalities adjacent to the C2 position of indoles.

1 Introduction

Indole alkaloids represent a significant class of natural products[1] owing to their unique polycyclic architectures and promising biological activities (Fig. 1A).[2–4] Numerous indole-derived or natural product-like compounds feature complex structures at the C2 and C3 positions of the indole ring;[5] however, functionalization at the C2 position remains difficult to achieve, prompting extensive research efforts in recent years. Recently, several approaches have been developed for indole C2 functionalization. One strategy involves acid- or oxidation-catalyzed Prins-type reactions,[6,7] such as employing CH_3SO_3H, CF_3COOH, HCl, H_2SO_4, or (1*S*)-(+)-camphor-10-sulfonic acid (CSA),[8] which may require stoichiometric amounts of acidic reagents. Another strategy involves transition metal-catalyzed cross-coupling reactions at the C2 position, using palladium[9] or copper[10] as catalysts, often in combination with ligands such as phosphines.[11] Photoredox-catalyzed dearomatization of indoles with amines,[12] palladium-/copper-catalyzed regioselective amination and chloroamination,[13] and acid-catalyzed activation of indolenine are also attractive synthetic routes.[14] Despite these excellent methods, practical and efficient strategies for the C2 functionalization of indoles are still highly desirable for affording diverse and complex indoles.

Cerium photocatalysis is well-known in inorganic chemistry, primarily through excitations that drive redox processes—reducing cerium from Ce(IV) to Ce(III) while oxidizing the coordinated ligand.[15–18] Zuo's group has designed excellent ligand-to-metal charge transfer (LMCT) strategies for hydroxyl group activation,[19] and the subsequently developed hydrogen atom transformation (HAT) model, which perfectly addressed challenges in δ-selective functionalization of alkanols.[20]

In our previous work, as demonstrated in Fig. 1B, we employed a cerium-mediated photocatalytic ligand-to-metal charge transfer (LMCT) strategy for activating indole alkanols (tryptophol) to generate alkoxy radicals. These radicals undergo regioselective intramolecular addition to the indole 2,3-alkene bond, triggering dearomatization and subsequent cyclization to afford furoindolines.[21]

[a]*Yunnan Key Laboratory of Research and Development for Natural Products, Key Laboratory of Medicinal Chemistry for Natural Resource (Ministry of Education), School of Pharmacy, School of Chemical Science and Technology, Yunnan University, Kunming 650091, China. E-mail: injun@ynu.edu.cn; beizhou@swfu.edu.cn*

[b]*Yunnan Provincial Key Laboratory of Wood and Bamboo Biomass Materials, Yunnan Provincial International Joint Research and Development Center for Green and Low-Carbon Utilization of Characteristic Wood and Bamboo Materials, Key Laboratory of Forest Resources Conservation and Utilization in the Southwest Mountains of China (Ministry of Education), International Joint-Research Center for Bio-Materials (Ministry of Science and Technology), College of Materials and Chemical Engineering, Southwest Forestry University, Kunming 650224, China*

[c]*Yunnan Key Laboratory of Breeding and Utilization of Resource Insects, Key Laboratory of Protection and Utilization of Insects (National Forestry and Grassland Administration), Research Center of Engineering and Technology of Characteristic Forest Resources (National Forestry and Grassland Administration), Institute of Highland Forest Science, Chinese Academy of Forestry, Kunming 650233, China*

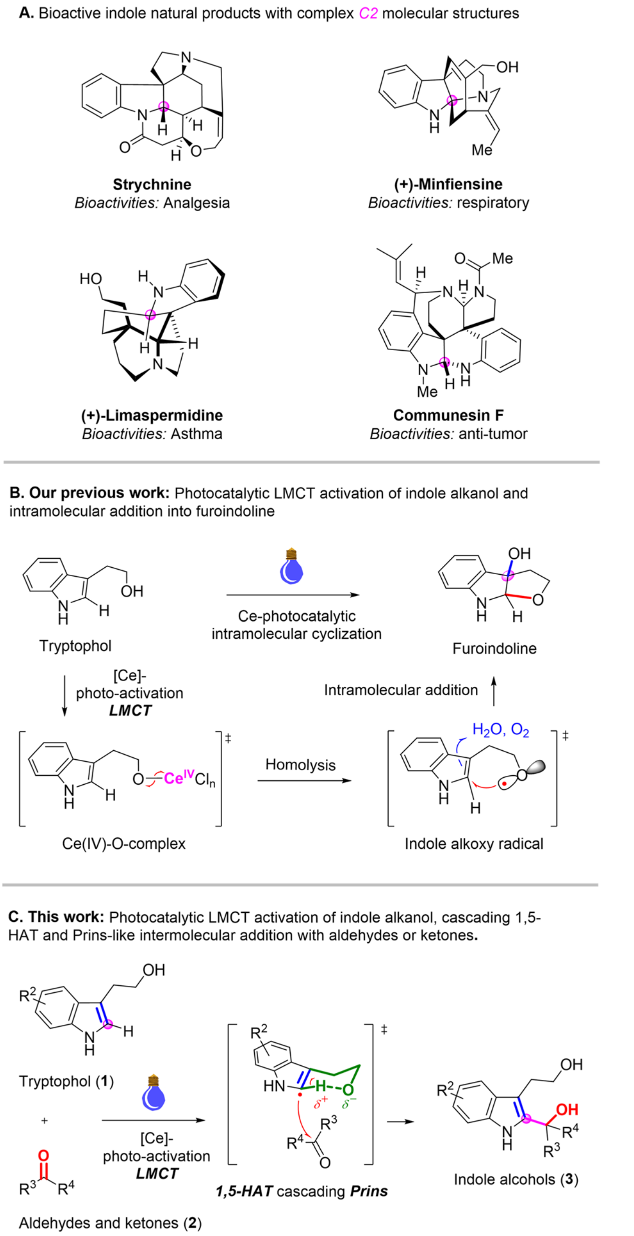

Fig. 1 (A) Indole natural products. (B) Our previous work: LMCT induced indole intramolecular reaction. (C) This work: LMCT induced indole intermolecular reaction.

Basing on the cerium-photocatalytic LMCT process, as illustrated in Fig. 1C, our work presents a further modification to this process for the δ-selective functionalization of indole alkanols. This approach involves the initiation of an intramolecular LMCT pathway, which activates indole-alkanols to generate indole alkoxy radicals. The generated alkoxy radical facilitates selective cleavage of the indole C2 sp^2 C–H bond through a 1,5-hydrogen atom transfer (1,5-HAT) mechanism, thereby producing a carbon radical at the indole C2 position. This reactive carbon radical subsequently undergoes nucleophilic addition to aldehydes or ketones, yielding secondary alcohols from aldehydes and tertiary alcohols from ketones.

2 Results and discussion

2.1. Basic photocatalytic synthesis reaction

In a typical photocatalytic reaction (Table 1), the DCM solution of tryptophol (**1**, 0.25 gram-scale), acetaldehyde (**2**, 1.0 equiv.) and $CeCl_3$ was irradiated by blue LED light with TBAC and TCE. The reaction was carried out in an Ar atmosphere at an ambient temperature. After 15 h, target indole alcohols (**3**) were isolated with a yield of 82%.

We conducted this reaction under different reaction conditions to examine the effect of the reaction parameters on the reaction yield. The experiment details and results are listed in Table 1. No nucleophilic addition products **2** were obtained without $CeCl_3$ (Table 1, entry 2).

When the reaction was performed without photo-irradiation, no alcohol product was obtained even at an elevated temperature (80 °C) for 24 h (Table 1, entry 3). The combination of TBAC and TCE was evaluated as the required additives for the reaction (Table 1, entry 4).

LEDs with different spectral bands, such as 365–370 nm, 395–400 nm, 410–415 nm, 460–465 nm, 520–525 nm, 590–595 nm, 620–625 nm, and blue light (18 W for all LEDs) were used for the reaction. The reaction irradiated by a shorter wavelength of light consumed the indole and aldehyde reactants but resulted in less targeted products, hence lower yield but larger conversion efficiency (Fig. 2).

The reaction under blue LED light (λ = 400 –480 nm) irradiation achieved the best yield (Table 1, entry 5).18 W LED light was chosen as the light source in further experiments. DCM was selected as the optimal reaction solvent, as the target product was not observed when THF, DMF, dioxane, or DMSO were used as solvents (Table 1, entries 6–9).

When DCM was replaced with a large amount of H_2O or a DCM/H_2O mixture (v/v, 1 : 1) was used as the reaction solvent, the target product was obtained with a slight decrease in yield (Table 1, entries 10–11). MeOH, acetone, and MeCN were also evaluated as reaction solvents, but afforded lower product yields (Table 1, entries 12–14).

The atmospheric conditions impacted the reaction greatly. When the reaction was conducted in an O_2 atmosphere, the yield was 42% (Table 1, entry 15), lower than in an Argon atmosphere. When the reaction time was extended from 1 h to 15 h and 20 h, the yield increased from 12% to 82% and 80%. It suggests that a longer reaction time than 15 h would slightly decrease the yield (Table 1, entries 16–21, the products were analyzed by GC-MS).

The above results suggest that $CeCl_3$, blue light, and argon are essential for this reaction. Since $CeCl_3$ is a visible-light radical photocatalyst, which involves a typical single electron transfer oxidation as reported in the literature, we tested other four photo-catalysts (Table 1, entries 22–25), tris[2-phenyl-pyridine]-iridium(III) (tris-Ir(ppy)$_3$), tris-(2,2′-bipyridine) ruthenium(II) dichloride (Ru(bpy)$_3$Cl$_2$), 2,4,5,6-tetrakis-(carbazol-9-yl)-1,3-dicyano-benzene (4CzIPN) and Rose Bengal. Ru(bpy)$_3$Cl$_2$ has a metal-polypyridyl complex structure similar to that of tris-Ir(ppy)$_3$. 4CzIPN[22] is a non-metal photocatalyst with a redox

Table 1 Effects of reaction parameters on the photocatalytic reaction

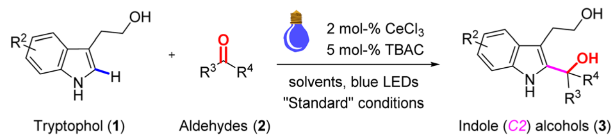

Entries	Variation from the standard reaction conditions[a]	Yield[b] (%)
1	None	82
2	No $CeCl_3$	—
3	No light, MeCN 80 °C for 24 h	—
4	No TBAC, neither TCE	Trace
5	Light wavelength, 365 nm, 395 nm, 410 nm, 460 nm, 520 nm, 590 nm, 620 nm	10–80
6	DCM replaced by THF	—
7	DCM replaced by DMF	—
8	DCM replaced by dioxane	—
9	DCM replaced by DMSO	—
10	DCM replaced by H_2O	25
11	DCM/H_2O (V/V, 1 : 1)	35
12	DCM replaced by MeOH	21
13	DCM replaced by acetone	49
14	DCM replaced by MeCN	70
15	Argon replaced by O_2	42
16	DCM, reaction time 1 h	12
17	DCM, reaction time 5 h	53
18	DCM, reaction time 8 h	70
19	DCM, reaction time 12 h	78
20	DCM, reaction time 15 h	82
21	DCM, reaction time 20 h	80
22	Tris-Ir(ppy)$_3$	—
23	Ru(bpy)$_3$Cl$_2$	—
24	4CzIPN	—
25	Rose bengal	—

[a] Standard reaction conditions: tryptophol (250 mg, 1.6 mmol, and 1.0 equiv.), acetaldehyde (1.0 equiv.), cerium(III) chloride ($CeCl_3$, 19.11 mg, 0.08 mmol, and 0.05 equiv.), tetrabutylammonium chloride (TBAC, 43.09 mg, 0.16 mmol, and 0.1 equiv.), 2,2,2-trichloro-ethanol (TCE, 23.18 mg, 0.16 mmol, and 0.1 equiv.) and dichloromethane (DCM, 20.0 mL) were added to a two-necked quartz flask. The reaction was carried out under the irradiation of blue LED lights (18 W and λ = 400 nm-480 nm) at room temperature in an argon (Ar) balloon atmosphere for 15 h and cooled using a fan. [b] Isolated yield were obtained by column chromatography using neutral alumina (Al_2O_3), and the yields were calculated after recycling the tryptophol reactant. "–" means no reaction and no target alcohol was observed.

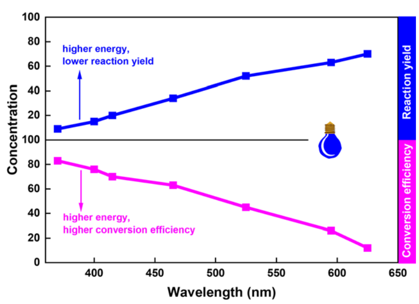

Fig. 2 Effect of light wavelength on reaction yield and conversion efficiency.

potential close to tris-Ir(ppy)$_3$, and it has a minimized energy gap between its singlet and triplet excited states. Rose Bengal is a general and widely used quinone-type natural photosensitizer. Under the same conditions, no reactions in these reaction conditions and no target product were observed in the reactions catalyzed by these four photocatalysts. These results indicate that a specific photoredox energy transformation is crucial for the indole C2 sp^2 C–H bond activation and the subsequent nucleophilic addition in this indole–aldehyde reaction.

To systematically evaluate the influence of the cerium oxidation state and counterion on catalytic activity, we tested a range of cerium-based compounds: Ce(SO$_4$)$_2$ (cerium(IV) sulfate), Ce(CF$_3$SO$_3$)$_3$ (cerium(III) triflate), Ce(CF$_3$SO$_3$)$_4$ (cerium(IV) triflate), Ce$_2$(CO$_2$)$_2$ (cerium(III) carbonate), and Ce(CH$_3$COO)$_3$ (cerium(III) acetate). None of these catalysts initiated the desired transformation under the established reaction conditions. In contrast, $CeCl_3$, whether anhydrous or hydrated, consistently delivered high reactivity and selectivity, confirming its unique suitability for this transformation.

We found that the chloride anion, supplied either by tetrabutylammonium chloride (TBAC) or 2,2,2-trichloroethanol (TCE), plays a critical role in enhancing reaction efficiency. In the absence of 5 mol% TBAC, the yield of the desired product dropped to 25%, with 56% of the starting material being

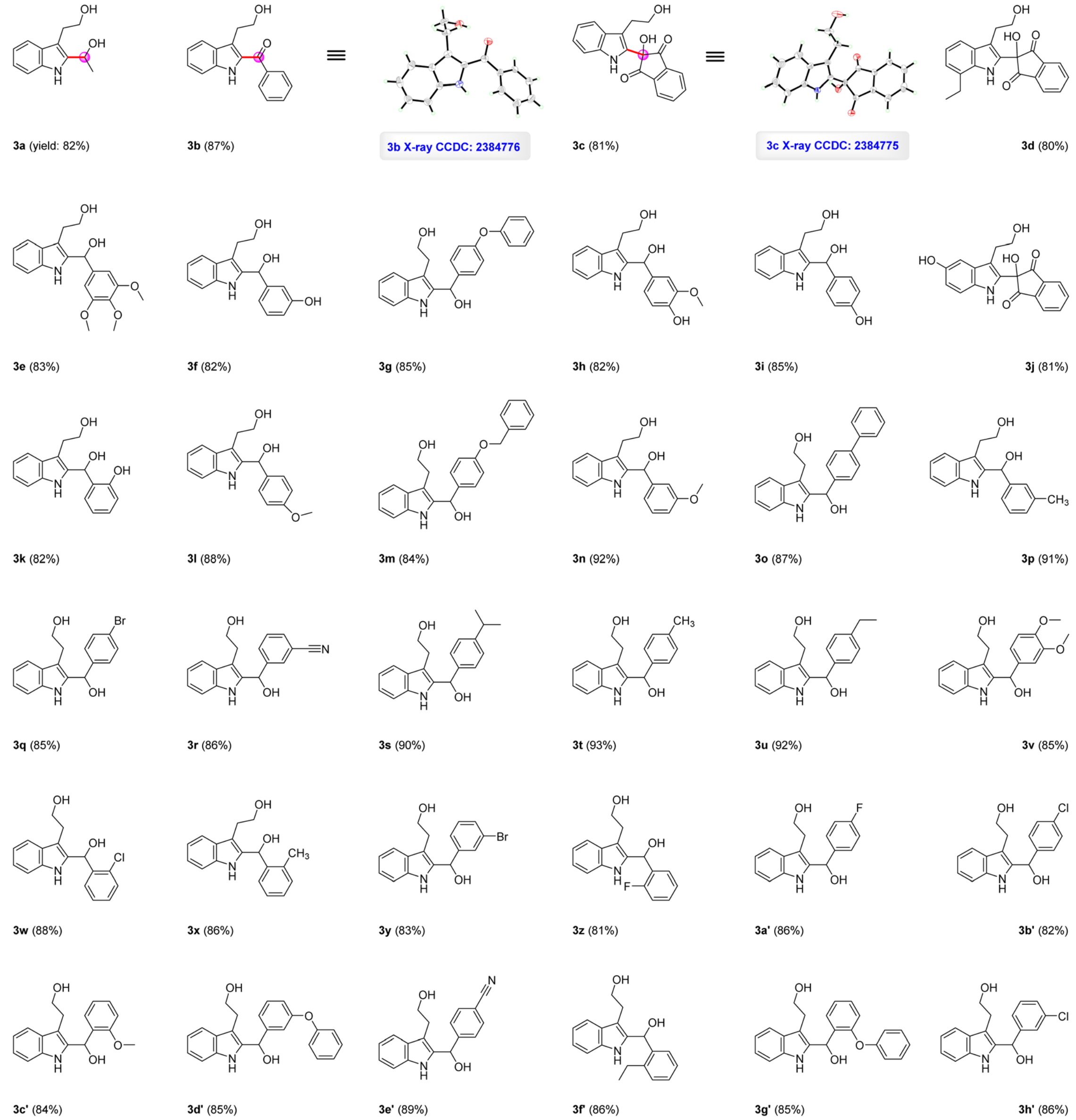

Fig. 3 Chemical structures of target products, along with their isolated yields. For comprehensive details on the reaction scope and experimental procedures, including ^{1}H-NMR, ^{13}C-NMR, CCDC, and X-ray crystallographic data, refer to SI.

recovered. Substituting TBAC with tert-butylammonium salts of hydroxide, acetate, bromide, or iodide led to consistently lower yields, underscoring the unique efficacy of chloride. Additionally, TCE serves a dual function, as a source of chloride and as a protic solvent that stabilizes the alkoxy radical intermediate during initiation.

The results presented above were obtained from the reaction employing tryptophol **1** and formaldehyde **2**. To evaluate the versatility of the reaction, a series of indoles, aldehydes, and ketones bearing diverse functional groups were systematically investigated, as illustrated in Fig. 3 (further details are provided in the ESI).

As exemplified by product **3b**, the alcohol formed adjacent to the indole C2 position undergoes further oxidation to the corresponding ketone, a consequence of the net oxidation process inherent to this transformation. When benzaldehyde was employed, nucleophilic addition of the indole C2 carbon radical to the aldehyde is followed by the elimination of an α-hydrogen atom.

Ninhydrin was also employed as the ketone substrate, resulting in the corresponding tertiary alcohol (**3d**). Benzaldehyde derivatives bearing specific substituents, such as hydroxy and halogen groups on the aromatic ring, were found to be suitable substrates for this transformation (*e.g.*, **3f** and **3y**). Furthermore, we have demonstrated that indole substrates containing a hydroxy group on the benzo ring are compatible with the reaction conditions, yielding the desired product in 81% yield (**3j**).

We further evaluated several aliphatic aldehydes, including formaldehyde (tested at two concentrations: 37% and 50%

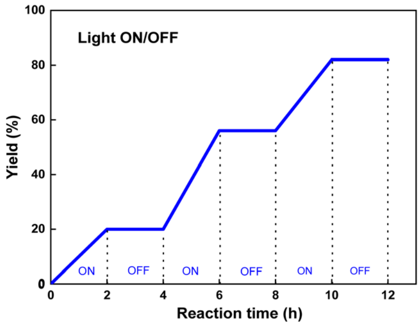

Fig. 4 Light ON/OFF experiments for the radical propagation test (the yield of indole alcohol product **2** was measured by GC analysis).

aqueous solutions); however, no target product was isolated. This outcome suggested that the reactivity of these aldehydes, particularly formaldehyde, was insufficient under the current reaction conditions to engage efficiently in the proposed transformation with indole.

In summary, for the substrate generality of this method, aldehydes and ketones, including linear aliphatic carbonyls, benzaldehydes, and ninhydrins, are broadly compatible with this method.

2.2. Investigation of the reaction mechanism

We further conducted a series of experiments to probe the reaction mechanism, such as light ON/OFF control, radical inhibition, and isotope-labeling experiments.

A light ON/OFF control experiment was conducted, and the yield of the indole alcohol product **2** was measured at different reaction times using gas chromatography (GC). As shown in Fig. 4, the yield was blocked immediately when the light was turned off. However, the reaction resumed when the light was turned on, indicating that constant light irradiation is essential for this transformation.

When conducted in the presence of 2,2,6,6-tetramethyl-1-oxylpiperidine (TEMPO), a stable oxyl radical, the photocatalytic reaction was seriously inhibited (Fig. 5). No reaction occurred when the reaction used other radical initiators, such as t-butylated hydroxytoluene (BHT) and tri-^{n}butyltin hydride (^{n}Bu$_3$SnH). They indicate that photocatalytic transformation is a radical reaction process.

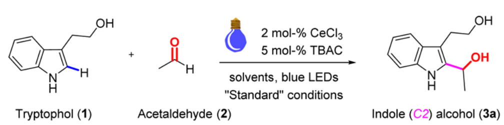

Scavenger	Yield 3
None	82%
TEMPO (2.0 equiv.)	–
BHT (2.0 equiv.)	–
^{n}Bu$_3$SnH (2.0 equiv.)	–

Fig. 5 Radical inhibition experiments. "–" means no target alcohol was observed.

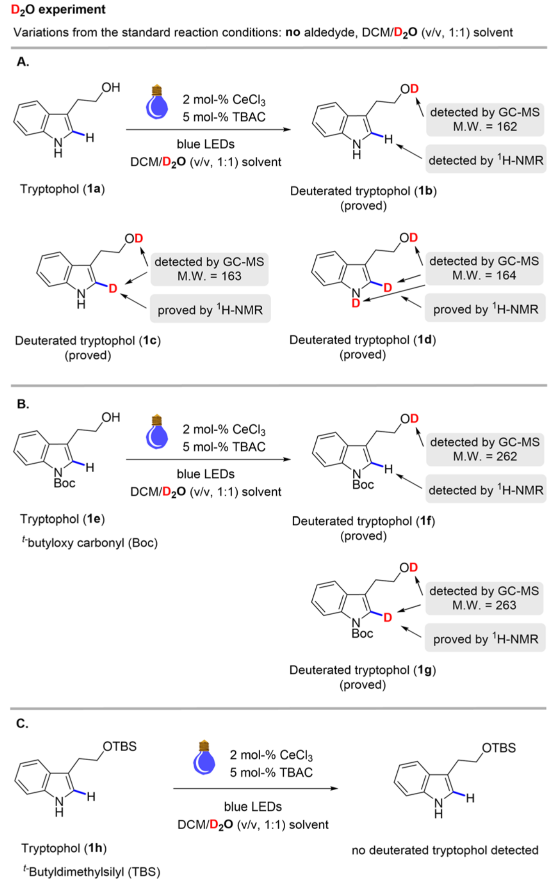

Fig. 6 Isotope experiments with DCM/D$_2$O solvents. (A) Tryptophol without any protection. (B) Tryptophol with a tert-butyloxycarbonyl (Boc) protection on nitrogen atom of indole. (C) Tryptophol with a tert-butyldimethylsilyl (TBS) protection on hydroxyl group.

The hydrogen atom transfer processes occurring during this photocatalytic radical reaction were monitored using **D$_2$O** as the solvent (Fig. 6). As shown in Fig. 6A, when the reaction was carried out with tryptophol in the absence of aldehyde and using a DCM/**D$_2$O** mixture (v/v, 1 : 1) as the solvent, deuterated tryptophol derivatives bearing a deuterated hydroxyl group (**1b**), a C2-deuterated product (**1c**), and an *N*-deuterated product (**1d**) were detected by GC-MS after approximately 15 hours. These findings indicate that both the hydroxyl group and the nitrogen atom on the indole ring are activated under these mild photocatalytic conditions, with selective cleavage of the sp^2 C2–H

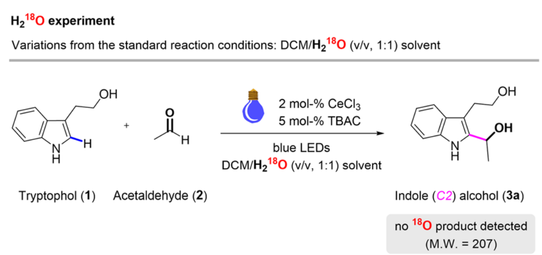

Fig. 7 Isotope-labeling experiments with H$_2$^{18}O.

bond taking place. As illustrated in Fig. 6B, when the nitrogen atom of the indole ring was protected with a tert-butyloxycarbonyl (Boc) group, both the deuterated hydroxyl-containing product (**1f**) and the C2-deuterated product (**1g**) were still observed. In contrast, as shown in Fig. 6C, when the hydroxyl group of tryptophol was protected with a tert-butyldimethylsilyl (TBS) group, no deuterated products were detected. These results demonstrate that the presence of a free hydroxyl group is essential for activation of the sp^2 C2–H bond in the indole moiety.

The oxygen atom transfer processes occurring during this photocatalytic radical reaction were monitored using $H_2^{18}O$ as the solvent (Fig. 7). When the reaction was conducted with both tryptophol **1** and aldehyde **2** as substrates in a DCM/$H_2^{18}O$ mixture (v/v, 1 : 1), no ^{18}O-labeled product was detected after 15 hours, indicating that both oxygen atoms in product **3a** originate from the substrates rather than from the solvent or the ambient atmosphere.

To probe the reaction mechanism, we hypothesize that, upon photoirradiation, the aldehyde first coordinates to the Ce(III) catalyst and undergoes single-electron reduction to generate a ketyl radical intermediate, and this ketyl radical then engages in radical coupling with indole to afford the target product. We evaluated a series of indole derivatives, as illustrated in Fig. 8, including unsubstituted indoles at C3 and indole alkanols lacking the hydroxyl group (substrates **1a–1g**) alongside alternative carbonyl partners (substrates **2**: ketones and aldehydes), all under the "standard reaction conditions". In all cases, no target product was obtained.

Notably, when substrate **1g** was employed with the indole nitrogen Boc-protected and the hydroxyl group of the indole alkanol left unprotected, the reaction also failed to yield the desired product. Collectively, these control experiments support the mechanistic hypothesis that activation of the indole alkanol (tryptophol) to generate an alkoxy radical is essential. This alkoxy radical is proposed to mediate hydrogen atom abstraction from the C2 position of the indole ring, thereby generating an indolyl radical that engages in C–C bond formation with the carbonyl substrate **2**.

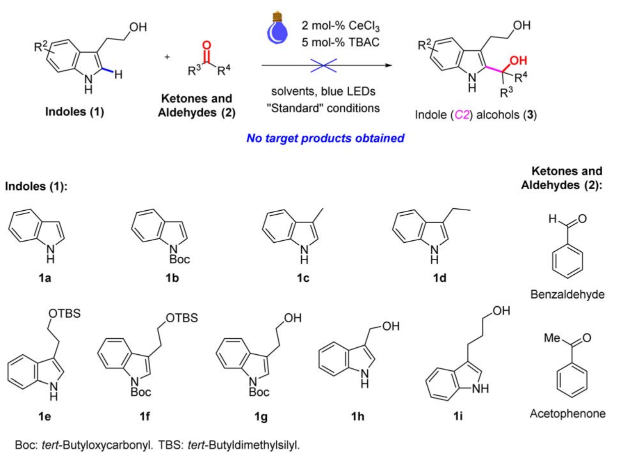

Fig. 8 Exploration of the reaction mechanism using various substrates.

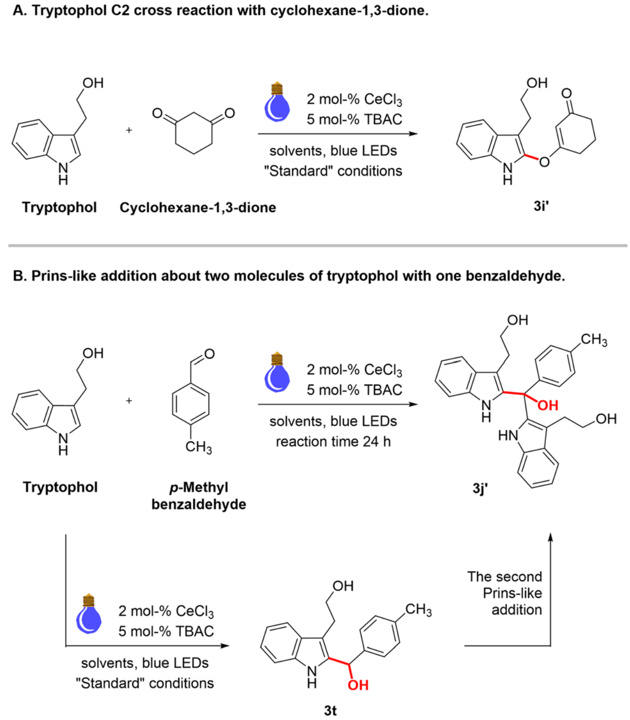

Fig. 9 Mechanism investigation experiments. (A) Cyclohexane-1,3-dione oxygen-reaction with tryptophol. (B) Prins-like addition about two molecules of tryptophol with one benzaldehyde.

Systematically varying the linker length is indeed an excellent strategy to probe the steric and conformational constraints governing the reactivity of the 1,n-HAT process, including 1,4-HAT, 1,5-HAT, and 1,6-HAT, and potentially reveal a side-chain length dependence in this transformation. To address this point, we evaluated substrate **1h** (bearing a methylene linker) and **1i** (bearing a propyl linker), both of which afforded trace amounts of the desired product under standard conditions.

We also conducted additional mechanistic investigations to probe the reactivity of the tryptophol C2 position, as shown in Fig. 9. Under standard reaction conditions (Fig. 9A), treatment of tryptophol with cyclohexane-1,3-dione afforded product **3i′**, featuring a new C–O bond between the C2 carbon of tryptophol and the carbonyl oxygen of cyclohexane-1,3-dione.

Building on the Prins-type reaction between tryptophol and *p*-methylbenzaldehyde—which yielded product 3 t (Fig. 9B)—we extended the reaction time from 15 h to 24 h and successfully isolated product **3j′**. This transformation involves sequential Prins-type additions at two distinct tryptophol C2 sites with the same benzaldehyde molecule, indicating that the tertiary alcohol moiety in 3 t undergoes further photocatalytic C-centered activation under LMCT catalysis.

2.3. Proposed reaction mechanism

Cerium-based photocatalysis has been established in inorganic chemistry, primarily through excitations that drive redox processes—reducing cerium from Ce(IV) to Ce(III) while oxidizing the coordinated ligand.[15–18] Subsequently, Zuo's group

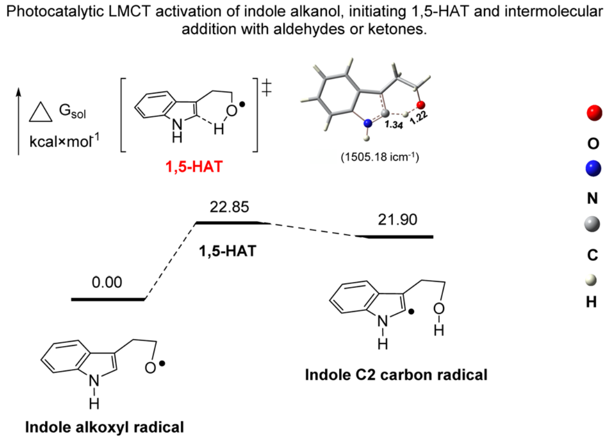

Fig. 10 Density functional theory (DFT) calculations for reaction energy barriers and pathways, potential energy surface (PES) and electrostatic potentials (ESP). Photocatalytic LMCT activation of indole alkanol, initiating the 1,5-HAT process for the intermolecular addition with aldehydes or ketones.

developed highly effective ligand-to-metal charge transfer (LMCT) strategies for hydroxyl group activation,[20,23] along with a subsequent hydrogen atom transfer (HAT) mechanism, which successfully addressed the challenges associated with δ-selective functionalization of alkanols.[19]

To elucidate how bond dissociation energies (BDEs) influence the reaction energy barriers and govern the hydrogen atom transfer (HAT) pathway, we performed DFT calculations, and the results are presented in Fig. 10. The DFT-calculated energy profile for the indole alkanol substrate and the corresponding transition state of the 1,5-HAT step revealed an activation barrier of 22.85 kcal mol^{-1}, demonstrating that the HAT pathway was kinetically accessible.

Inspired by the work that the cerium–hydroxyl coordination complex (–OH–[Ce]) can be effectively photoexcited under visible light,[24] leading to homolytic cleavage of the Ce(IV)–OR bond and generation of a highly reactive alkoxy radical,[22,25] we hypothesized that, as illustrated in Fig. 11, employing an indole alkanol (tryptophol **1**) in this ligand-to-metal charge transfer (LMCT) excitation process (**M2**) would enable the resulting indole alkoxy radical to initiate selective cleavage of the indole C2 sp^2 C–H bond (**M3**) *via* a 1,5-hydrogen atom transfer (1,5-HAT) pathway (**M4**), thereby forming a carbon-centered radical at the C2 position (**M6**). This generated carbon radical could then undergo nucleophilic addition to aldehydes or ketones (**M7**), affording secondary alcohols (**3**) from aldehydes and tertiary alcohols from ketones. We also observed that the alkoxy radical intermediate (**M7**) could undergo further side reactions, such as protonation, oxidation, and other nucleophilic additions, leading to minor byproducts distinct from the dominant Prins-like cyclization pathway.

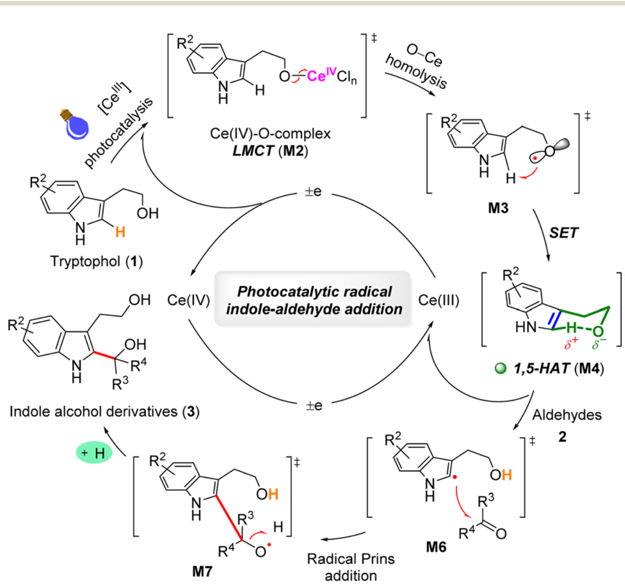

Fig. 11 Reaction mechanism.

3 Conclusion

In summary, basing on a remote-control functionalization strategy, we developed a general approach for the excitation of indole alkanols *via* an alkoxy-radical-mediated ligand-to-metal charge transfer (LMCT) photocatalysis process. This method provides a mild and efficient protocol for activating the indole C2 sp^2 C–H bond through a 1,5-hydrogen atom transfer (1,5-HAT) pathway, enabling nucleophilic addition of the resulting carbon-centered radical at the C2 position to aldehydes or ketones, thereby affording secondary alcohols from aldehydes and tertiary alcohols from ketones. This work presents an efficient photocatalytic radical-based transformation analogous to the Prins reaction and offers a practical synthetic route for constructing alcohol functionalities adjacent to the C2 position of indoles, which holds great potential for the synthesis of complex indole-containing pharmaceuticals and polymeric materials.

4 Experimental section

4.1. General procedure for basic photocatalytic synthesis reaction

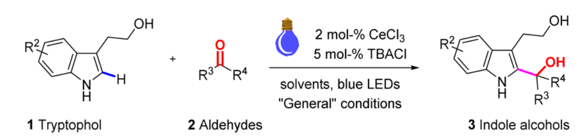

In an oven-dried quartz flask (50 mL) equipped with a stir bar, tryptophol (250 mg, 1.6 mmol, 1.0 equiv.), aldehydes (1.0 equiv.), cerium(III) chloride (19.11 mg, 0.08 mmol, 0.05 equiv.), tetrabutylammonium chloride (43.09 mg, 0.16 mmol, 0.1 equiv.), 2,2,2-trichloro-ethanol (23.18 mg, 0.16 mmol, 0.1 equiv.) and dichloromethane (DCM, 20.0 mL) were combined and added. The reaction was conducted under an argon atmosphere using an Ar balloon. The reaction mixture was stirred and illuminated by blue LED lights at room temperature for 15 h and cooling by a fan. Using TLC, with UV light as a visualizing agent, the reaction was monitored, and an ethanolic solution of phosphomolybdic acid, cerium sulfate, and heat as a developing agent. When the reactant material was no longer decreased, the solution was extracted with DCM (6 × 10 mL) and H_2O (3 × 10 mL). The combined organic layer was dried with Na_2SO_4 and filtered. The solvent was removed with a rotary evaporator. The pure product was obtained by flash chromatography on neutral alumina (Al_2O_3, Merck KGaA, 70–230 mesh, and pH = 6.8–7.8) using ethyl acetate and petroleum ether (1 : 15, vol/vol) as the eluent solvents. The target product was obtained. The isolated yields of all products were obtained by column chromatography.

Author contributions

Jun Lin, Bei Zhou, and Guanben Du: conceptualization, project administration, and funding acquisition. Lanxiang Liu, Yunfeng Tao, Menghan Chu, and Xiaojian Zhou: investigation and methodology. Bei Zhou, and Lanxiang Liu: writing – review & editing.

Conflicts of interest

The authors declare no known competing financial interests or personal relationships that could have appeared to influence the work reported in this paper.

Data availability

The authors declare that all data supporting the findings of this study are available within the manuscript and supplementry information (SI) files and are available from the corresponding author upon reasonable request.

Supplementary information: general photocatalysis experiment, characterization data, NMR spectra, computational experiments data, and X-ray crystal structure experiments data. See DOI: https://doi.org/10.1039/d5ra09558a.

Acknowledgements

Funding support from the National Natural Science Foundation of China (No. 32260363 and 32471797), Yunnan Provincial International Joint Research and Development Center for Green and Low-Carbon Utilization of Characteristic Wood and Bamboo Materials, Yunnan "Xingdian Talents Support Program"-Innovation Team Special Project (*No.* 202605AS350004), the Yunnan Fundamental Research Project (No. 202301AT070180), the Yunnan province Xingdian Talents Support Plan (Li Shuai 2024 and Xiaojian Zhou 2023), the Programme of Introducing Talents of Discipline to Universities (the 111 Project, No. D21027), Foreign Experts Work Station (No. 202305AF150006), and Yunnan Province Academician Free Exploration Fund (No. 202405AA350027) is acknowledged. The authors thank the Shiyanjia Lab (https://www.shiyanjia.com/) for the experimental analysis tests and Hangzhou Yanqu Information Technology Co., Ltd for the computational work. Chemical reagents (including purified water) were obtained from commercial suppliers (Sigma-Aldrich, Adamas, Shanghai Titan Technology Co., Ltd, Adamas *et al.*).

Notes and references

1 T. P. Singh and O. M. Singh, *Mini-Rev. Med. Chem.*, 2018, **18**, 9–25.
2 D. C. Holland and A. R. Carroll, *Nat. Prod. Rep.*, 2023, **40**, 1595–1607.
3 S. E. O'Connor and J. J. Maresh, *Nat. Prod. Rep.*, 2006, **23**, 532–547.
4 Z. Chang, Y. Wang, Y. Li, J. Ye, S. Cui, X. Li, Y. Tao, B. Zhou and H. Lei, *New J. Chem.*, 2024, **48**, 12348–12354.
5 Y. F. Tao, Y. J. He, J. Z. Ye, X. Yang, Y. Y. Yang, G. G. Xie, L. X. Liu, G. B. Du, H. Zhang and B. Zhou, *New J. Chem.*, 2021, **45**, 15336–15343.
6 Y. Li, J. Ye, Q. Chen, J. Tao, Y. Tao, Y. Wang, L. Liu, B. Zhou, X. Zhou and G. Du, *New J. Chem.*, 2025, **49**, 8800–8809.
7 B. Zhou, Y. J. He, Y. F. Tao, L. X. Liu, M. Hu, Z. H. Chang, H. Lei, J. Lin, T. Lin and G. B. Du, *Green Chem.*, 2022, **24**, 2859–2870.
8 E. Y. L. Hui, B. Rout, Y. S. Tan, C. S. Verma, K. P. Chan and C. W. Johannes, *Org. Biomol. Chem.*, 2018, **16**, 389–392.
9 C. Shao, G. Shi, Y. Zhang, S. Pan and X. Guan, *Org. Lett.*, 2015, **17**, 2652–2655.
10 X. Wang, S. Zhao, J. Liu, D. Zhu, M. Guo, X. Tang and G. Wang, *Org. Lett.*, 2017, **19**, 4187–4190.
11 B. Zhou, Y. F. Tao, Y. J. He, L. X. Liu, Z. H. Chang, X. H. Li, T. Lin and G. B. Du, *Green Chem.*, 2023, **25**, 196–210.
12 J. Wang, G. Wei, J. Luo, J. Cheng, D. Zhang, X. Chen, F. Tan, T. Yang, H. Li and B. Huang, *Org. Lett.*, 2025, **27**, 10465–10470.
13 X. Y. Liu, P. Gao, Y. W. Shen and Y. M. Liang, *Org. Lett.*, 2011, **13**, 4196–4199.
14 T. Abe and K. Yamada, *Org. Lett.*, 2016, **18**, 6504–6507.
15 S. S. Lande and J. K. Kochi, *J. Am. Chem. Soc.*, 1968, **90**, 5196–5207.
16 A. Vogler and H. Nikol, *Pure Appl. Chem.*, 1992, **64**, 1311–1317.
17 C. Tanielian, *Coordin. Chem. Rev.*, 1998, **178**, 1165–1181.
18 A. Juris, P. Ceroni and V. Balzani, in *Photochemistry and Photophysics: Concepts, Research, Applications*, 2014.
19 J. J. Guo, A. H. Hu, Y. L. Chen, J. F. Sun, H. M. Tang and Z. W. Zuo, *Angew. Chen.-Int. Edit.*, 2016, **55**, 15319–15322.
20 Y. Xu and G. B. Dong, *Chem*, 2020, **6**, 10–11.
21 L. Liu, Y. Tao, Y. Song, X. Zhou, G. Du, B. Zhou and J. Lin, *New J. Chem.*, 2026, **50**, 4264–4270.
22 H. Uoyama, K. Goushi, K. Shizu, H. Nomura and C. Adachi, *Nature*, 2012, **492**, 234–235.
23 A. Vogler and H. Kunkely, *Inorg. Chim. Acta*, 2006, **359**, 4130–4138.
24 A. H. Hu, J. J. Guo, H. Pan, H. M. Tang, Z. B. Gao and Z. W. Zuo, *J. Am. Chem. Soc.*, 2018, **140**, 1612–1616.
25 J. Friedrich, D. Schneider, L. Bock, C. Maichle-Mössmer and R. Anwander, *Inorg. Chem.*, 2017, **56**, 8114–8127.